Structural Durability & Health Monitoring

Tech Science Press

https://doi.org/10.32604/sdhm.2026.080823

ARTICLE

Experimental Study on the Tensile Performance of Fully Grouted Sleeve Connections after High-Temperature Exposure

Ning Lin*

Fuzhou Municipal Infrastructure Safety Center for Buildings and Civil Works, Fuzhou, China

*Corresponding Author: Ning Lin. Email: linning0591@163.com

Received: 15 February 2026; Accepted: 07 April 2026; Published: 24 August 2026

ABSTRACT: The fully grouted sleeve connection is a key joint type in precast concrete structures. Its mechanical performance after high-temperature exposure is critical for the post-fire safety assessment of these structures. This paper experimentally investigates the influence of different peak temperatures on the tensile performance of fully grouted sleeve connections. A total of 36 fully grouted sleeve specimens, 36 single rebar specimens, and their corresponding grout cubes were prepared. All specimens were heated to the target temperatures and then cooled naturally. Afterwards, static tensile tests and compressive strength tests were performed. The results show that, compared to the strength at 25°C, the strength decreased by 43% at 600°C. The yield strength and ultimate strength of the steel rebar decreased by 17.2% and 10.5%, respectively, at 600°C. Below 600°C, all the fully grouted sleeve connections experienced tensile fracture of the rebar. At 600°C, the failure mode changed to pull-out failure. The load-displacement curves show that below 400°C, specimens are ductile, but at 600°C, the yield plateau decreases or vanishes. Based on the experimental data, predictive models for the yield stress and ultimate stress of the connections were established. A recommendation for the bond strength parameter k was also proposed, suggesting that a value of k > 1.79 can prevent pull-out failure. These findings provide an experimental basis and theoretical reference for the safety assessment of precast structures after fire.

KEYWORDS: Fully grouted sleeve; post-high-temperature; tensile performance; failure mode; bond strength; precast concrete structure

1 Introduction

Precast concrete (PC) structures have advantages over cast-*in-situ* concrete structures, including high construction quality, a high degree of industrialization, short construction periods, and reduced environmental pollution. The grouted sleeve connection, a type of joint in PC structures, has been used for over 40 years. In a grouted sleeve connection, steel rebars are placed inside a metal sleeve. This process creates a connection that transfers forces between the sleeve and the rebars. During load transfer, the load is passed from the rebar to the grout through bond action. The load then moves from the grout to the sleeve. The same mechanism transfers the load to the rebar on the other end. Similar to the role of conventional rebars, grouted sleeve joints are primarily subjected to tensile and compressive loads. Failure typically occurs when the tensile stress in the joint exceeds its peak value [1].

Fire is an extreme disaster that can cause severe damage to precast structures and their connections [2,3]. Post-earthquake fires pose a particularly significant threat to precast concrete structures and are currently a research focus. Under high temperatures, the mechanical properties of the grout and the rebar-sleeve interface can degrade significantly. Such deterioration can result in a decreased load-bearing capacity of the connection or even cause it to fail [4–6]. Therefore, there is a critical need for thorough research into the tensile performance of fully grouted sleeve connections after exposure to high temperatures.

Existing research has widely focused on various aspects of grouted sleeve connections. These include their mechanical behavior at room temperature [7], the effects of different grouting defects [8–10], and their seismic performance in corrosive environments. However, although research on grouted sleeve connections at high temperatures has reached the experimental stage, more studies are still needed [11]. Li et al. [8] indicates that after exposure to high temperatures, the compressive strength of grouted sleeve splices and the mechanical properties of the rebars significantly decline, with increasing defect rates and temperatures leading to a shift in the failure mode from rebar fracture to rebar pull-out.

High temperatures significantly affect the properties of building materials like concrete and steel rebar [12]. The study by Ma et al. [13] indicates that the bearing capacity of the reinforcement and semi-grouting sleeve connections shows little change under temperatures below 400°C. However, significant reductions in bearing capacity occur at temperatures above 600°C. Liu et al. [14] conducted a systematic analysis of the tensile behavior of half-grouted sleeve connections finding that when the peak temperature reached 800°C, the flexural and compressive strengths decreased by 82.1% and 56.3%, respectively. Li et al. [15] simulated building fires to explore the impact of different concrete cover thicknesses on the performance of grouted sleeve connections after high temperatures. They also considered factors such as peak temperature (200°C–800°C) and cooling method (natural cooling and water cooling).

Recent studies mainly concentrate on various factors that influence the tensile performance of grouted sleeve connections (GSCs), such as anchorage length, pre-damage state, and temperature [16]. For example, Zhang et al. [5] examined the influence of different anchorage lengths, pre-damage methods (monotonic and cyclic loading), and exposure temperatures ranging from 20°C to 800°C on the performance of grouted sleeve connections (GSCs). Their findings revealed that GSCs tend to exhibit increased brittleness at elevated temperatures. Similarly, Yi et al. [16] investigated the impact of inadequate anchorage lengths and high temperatures (100°C, 300°C, and 500°C) on the mechanical properties of grouted sleeve connections (GSCs) through monotonic and cyclic tensile tests.

Previous research clearly indicates that elevated temperatures negatively affect the performance of steel rebars and sleeve connections, which in turn governs the post-fire or post-high-temperature performance of PC structures. However, most existing investigations have addressed either the connection assembly or its constituent materials in isolation, and very few have provided a single dimensionless parameter that can be directly used to prevent bond failure in design practice. To bridge this gap, the present study contributes in four respects. (i) A synchronised triple-component experimental campaign was carried out on 36 fully grouted sleeve specimens, 36 single rebar coupons, and the corresponding grout cubes, all subjected to the same thermal histories at 25°C, 200°C, 400°C, and 600°C. The parallel design enables a decoupled analysis of bond-side and material-side degradation. (ii) A piecewise predictive model for the yield and ultimate stresses of fully grouted sleeve connections is proposed, with a transition temperature at 400°C that coincides with the dehydration window of calcium silicate hydrate (C–S–H) gel, giving the model a clear mechanistic basis rather than purely empirical fitting. (iii) An engineering-applicable design criterion, expressed as a dimensionless bond-strength coefficient $k > 1.79$, is distilled from the experimental data and is intended to be incorporated directly into post-fire safety-assessment workflows for precast joints. (iv) The diameter-independence of the post-high-temperature mechanical response is verified across the 12–16 mm range commonly used in engineering, providing a rational basis for unified assessment procedures. Together, these contributions provide both quantitative tools and design-oriented criteria for the fire-resistant evaluation of precast joints.

2 Experimental Programs

2.1 Raw Materials

The raw materials for the experiment included steel rebars, sleeves, and grout. The steel rebars were HRB400 grade hot-rolled ribbed bars with diameters of 12, 14, and 16 mm. The sleeves were fully grouted sleeves made of Q45 steel. The specifications used were D12, D14, and D16. The sleeves had a hollow cylindrical shape, and all their parameters met the requirements of JG/T 398 [17]. The fully grouted sleeve is shown in Fig. 1. C80 high-strength, non-shrinkage grout was selected as the bonding material inside the sleeves. It was prepared according to the manufacturer's recommended mix ratio, which was 3.6 L of water to 25 kg of grout. All materials were produced by commercial suppliers and are available on the market.

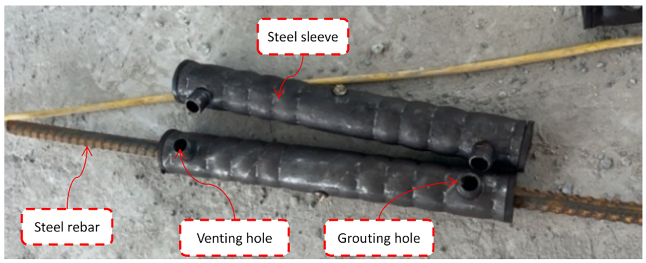

Figure 1: Reinforcing steel sleeve.

2.2 Specimen Design

The objective of this study was to measure the impact of varying temperatures on the mechanical performance of fully grouted sleeve connections. It also sought to clarify their performance degradation characteristics under heat. The goal was to provide an experimental basis for safety assessments after exposure to high temperatures or fire. To achieve this, specimens were subjected to four different temperature treatments: room temperature (25°C), 200°C, 400°C, and 600°C. After the heat treatment, the specimens underwent compressive and tensile performance tests. The specimen numbering is shown in Table 1. In the numbering system, 'C' represents the grout strength, 'R' represents the rebar diameter, and 'T' represents the temperature. For example, 'C80-T200' denotes a grout cube specimen made with C80 grout and heated to 200°C. 'C80-R12-T200' refers to a fully grouted sleeve connection specimen that uses C80 grout and a 12 mm diameter rebar, and it was heated to 200°C. The designation 'R12-T200' indicates a single rebar specimen with a 12 mm diameter, tested after exposure to 200°C.

Table 1: Specimen samples under different temperature conditions.

Specimen ID	Rebar Diameter (mm)	Temperature (°C)	Anchorage Depth at Grouting Inlet (mm)	Anchorage Depth at Grout Outlet (mm)
C80-R12-T25	12	25	96	136
C80-R12-T200	12	200	96	136
C80-R12-T400	12	400	96	136
C80-R12-T600	12	600	96	136
C80-R14-T25	14	25	112	136
C80-R14-T200	14	200	112	136
C80-R14-T400	14	400	112	136

(Continued)

Table 1 (continued)

Specimen ID	Rebar Diameter (mm)	Temperature (°C)	Anchorage Depth at Grouting Inlet (mm)	Anchorage Depth at Grout Outlet (mm)
C80-R14-T600	14	600	112	136
C80-R16-T25	16	25	128	136
C80-R16-T200	16	200	128	136
C80-R16-T400	16	400	128	136
C80-R16-T600	16	600	128	136

As specified in the standard JG/T 398 [17], the anchorage length of the rebar on the grouting inlet side was set to eight times the diameter of the rebar. The anchorage length of the rebar on the grout outlet side was determined by the maximum depth of the sleeve. The corresponding rebar anchorage depths are shown in Table 1. The specific configurations of the single rebar specimens and the fully grouted sleeve connections are detailed in Fig. 2.

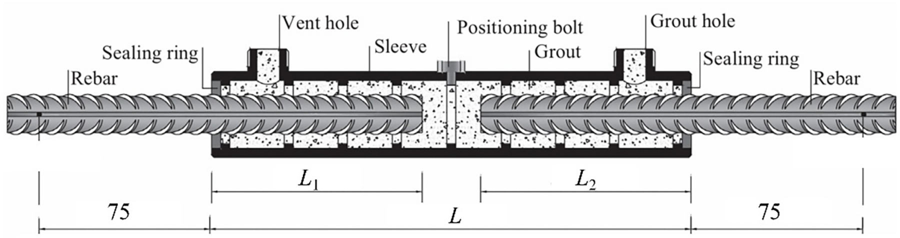

Figure 2: Configuration of the fully grouted sleeve connection.

2.3 Specimen Preparation

Mortar is mixed with water at the designed ratio until uniform. It is used to make connection specimens and 70 mm × 70 mm × 70 mm test cubes. After pouring, the specimens are vibrated for 2 min, sealed with polyethylene film, and cured at room temperature for 24 h. Then, they are moved to a standard curing environment (20 ± 2°C, humidity ≥ 95%) for 28 days.

To prepare the fully grouted sleeve specimens, sealing rings were first installed on the pre-cut rebars. The rebars with the sealing rings were then inserted into the sleeve from both ends. The openings of the sleeve were sealed by the rings, and the rebars were carefully centered. The assembled connector before grouting is shown in Fig. 3a.

Once the rebars and sleeve were secured, the prepared grout was injected into the sleeve from the bottom grouting inlet using a grouting pump. Pumping was stopped once grout was observed flowing continuously from the top grout outlet. The grouting inlet and outlet were then immediately sealed with foam plugs. The completed fully grouted sleeve connection is shown in Fig. 3b. These specimens were cured at room temperature for 28 days before being used for the subsequent mechanical performance tests.

After curing and heat treatment, grout cubes underwent axial compression tests to assess the impact of high temperatures on their compressive strength. Fully grouted sleeve connection specimens were tested for tensile strength, with sleeve specifications matching the rebar diameters.

(**a**) Before grouting (**b**) After grouting

Figure 3: The fully grouted sleeve connector with steel bars.

2.4 Heating Procedure and Loading Test

The specimens were placed in a high-temperature furnace and aligned for uniform heating (see Fig. 4a). They were heated to 100°C at a rate of 10°C/min and held at that temperature for 1 h. Then, they were heated to the peak temperature at the same rate and maintained there for 1 h.

(**a**) Heating Device (**b**) Loading test setup

Figure 4: Heating and loading test of connector.

The experiment utilized the temperature control system built into the heating furnace for temperature regulation. Temperature sensors were placed in the central area of the furnace, and a closed-loop feedback control was employed to ensure that the temperature rise curve met the specified requirements. Additionally, an independent high-temperature thermometer was used to calibrate the temperature at various points within the furnace, ensuring that the specimens were in a uniform thermal environment.

After the heat treatment, the specimens were removed from the furnace and allowed to cool naturally to room temperature before undergoing load tests. The loading test setup for the connectors is shown in Fig. 4b. During the loading test, a tensile rate of 5 mm/min was applied, and loading was continued until the specimen experienced fracture or pull-out failure. The displacement data during the loading process was automatically collected using the displacement sensor integrated into the tensile testing machine.

3 Results and Discussion

3.1 Compressive Strength of Grout Cubes after High Temperatures

After high-temperature exposure, the grout cubes were cooled to room temperature before compression testing. Table 2 shows the results. The compressive strength decreased as the peak temperature rose, aligning with Zhu et al. [18]. At 200°C, the strength dropped by 16%, at 400°C by 29%, and at 600°C by 43%, all compared to room temperature.

Table 2: Strength values of grouting test blocks.

Specimen ID	Compressive Strength (MPa)	Average (MPa)
C80-T25-1	89.3	
C80-T25-2	86.2	86.97
C80-T25-3	85.4	
C80-T200-1	72.6	
C80-T200-2	75.4	72.73
C80-T200-3	70.2	
C80-T400-1	60.6	
C80-T400-2	63.4	61.73
C80-T400-3	61.2	
C80-T600-1	48.6	
C80-T600-2	51.3	49.27
C80-T600-3	47.9	

To better characterise the underlying degradation mechanism, the temperature-normalised strength loss of the grout is examined in three temperature intervals. The average rate of strength loss is 0.0808 MPa/°C between 25°C and 200°C, decreases to 0.0550 MPa/°C between 200°C and 400°C, and re-accelerates to 0.0623 MPa/°C between 400°C and 600°C. The non-monotonic profile, in particular the re-acceleration above 400°C, is consistent with the dehydration of calcium silicate hydrate (C–S–H) gel and the decomposition of $Ca(OH)_2$ that are reported to occur in the 400–500°C range. This mechanistic interpretation, rather than the headline 43% drop alone, supports the choice of 400°C as the transition point of the predictive model proposed later in Section 3.5.

3.2 Tensile Strength of Rebars after High Temperatures

The yield strength and ultimate strength of rebars after high temperature are shown in Fig. 5. To evaluate the statistical significance of the experimental variables, a two-way analysis of variance (ANOVA) was performed. The results indicate that temperature had a statistically significant impact on both yield strength ($p = 0.0025$) and ultimate strength ($p < 0.001$). Regarding the rebar diameter, it exhibited no significant influence on the yield strength ($p = 0.071$), whereas its effect on the ultimate strength was found to be highly significant ($p < 0.001$), suggesting that specimen dimensions play a more critical role during the late-stage plastic deformation and fracture. Compared to the room temperature (25°C) condition, the average yield strength decreased by 9.0%, 14.3%, and 17.2% at 200°C, 400°C, and 600°C, respectively. Similarly, the ultimate strength decreased by 4.8%, 9.0%, and 10.5% at these respective temperatures. This phenomenon is primarily attributed to the microstructural degradation of the rebar material that occurs at high temperatures [19,20].

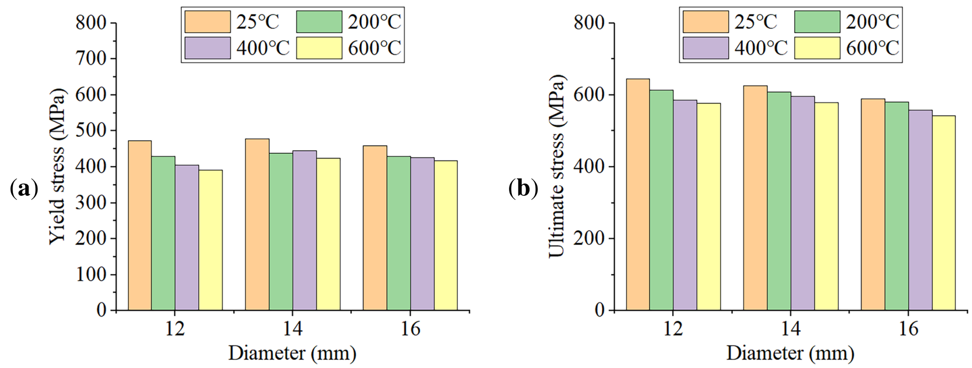

Figure 5: Rebar strength test values: (**a**) yield strength; (**b**) ultimate strength.

A more diagnostic indicator of post-high-temperature ductility is the strain-hardening ratio (f_n/f_y), which reflects the reserve of the rebar against fracture beyond yielding. Computed from the present data, this ratio decreases monotonically from 1.36 at 25°C, to 1.32 at 200°C, 1.30 at 400°C, and 1.28 at 600°C, an overall reduction of approximately 5.9%. Because the yield strength deteriorates faster than the ultimate strength, the difference between the two narrows progressively with temperature. From an engineering viewpoint, this narrowing reduces the ductility margin available for plastic redistribution in precast joints during a post-fire seismic event, which is a critical concern that has not been quantified in most existing studies of grouted sleeve connections.

3.3 Failure Modes and Breakpoint Locations

Table 3 shows the failure modes from the pull-out tests of fully grouted sleeve connectors after high-temperature exposure. There are two main modes: tensile fracture of the rebar (Fig. 6) and rebar pull-out from the sleeve (Fig. 7). The failure mode depends on the bond strength between the grout and the rebar, as well as the rebar's ultimate tensile strength.

Table 3: Test results of fully grouted sleeve after high temperature.

Specimen ID	Failure Mode	F_y (kN)	F_u (kN)	F_y (kN)	F_u Average (kN)
C80-R12-T25-1	Fracture	50.41	69.38		
C80-R12-T25-2	Fracture	49.86	66.37	50.81	69.04
C80-R12-T25-3	Fracture	52.16	71.38		
C80-R12-T200-1	Fracture	48.92	66.39		
C80-R12-T200-2	Fracture	50.42	69.39	50.18	68.62
C80-R12-T200-3	Fracture	51.21	70.08		
C80-R12-T400-1	Fracture	47.14	68.82		
C80-R12-T400-2	Fracture	41.54	67.38	45.51	67.53
C80-R12-T400-3	Fracture	47.86	66.38		
C80-R12-T600-1	Fracture	26.28	48.08		
C80-R12-T600-2	Pull-out	31.08	31.25	29.51	43.47
C80-R12-T600-3	Fracture	31.18	51.08		

(Continued)

Table 3 (continued)

Specimen ID	Failure Mode	F_y (kN)	F_u (kN)	F_y (kN)	F_u Average (kN)
C80-R14-T25-1	Fracture	72.14	94.28	73.04	96.47
C80-R14-T25-2	Fracture	76.24	102.07		
C80-R14-T25-3	Fracture	70.75	93.07		
C80-R14-T200-1	Fracture	64.06	91.68	66.14	94.18
C80-R14-T200-2	Fracture	68.29	95.52		
C80-R14-T200-3	Fracture	66.06	95.33		
C80-R14-T400-1	Fracture	61.93	81.31	60.95	84.74
C80-R14-T400-2	Fracture	58.58	84.15		
C80-R14-T400-3	Fracture	62.34	88.77		
C80-R14-T600-1	Fracture	42.83	62.96	40.35	62.45
C80-R14-T600-2	Fracture	41.58	65.56		
C80-R14-T600-3	Pull-out	36.65	58.82		
C80-R16-T25-1	Fracture	83.31	118.78	85.06	119.39
C80-R16-T25-2	Fracture	90.75	119.32		
C80-R16-T25-3	Fracture	81.13	120.06		
C80-R16-T200-1	Fracture	81.51	113.94	80.38	115.55
C80-R16-T200-2	Fracture	81.12	117.08		
C80-R16-T200-3	Fracture	78.52	115.62		
C80-R16-T400-1	Fracture	80.75	109.81	79.96	111.42
C80-R16-T400-2	Fracture	81.82	111.64		
C80-R16-T400-3	Fracture	77.32	112.81		
C80-R16-T600-1	Fracture	45.61	91.77	56.56	89.04
C80-R16-T600-2	Pull-out	63.77	81.58		
C80-R16-T600-3	Fracture	60.31	93.76		

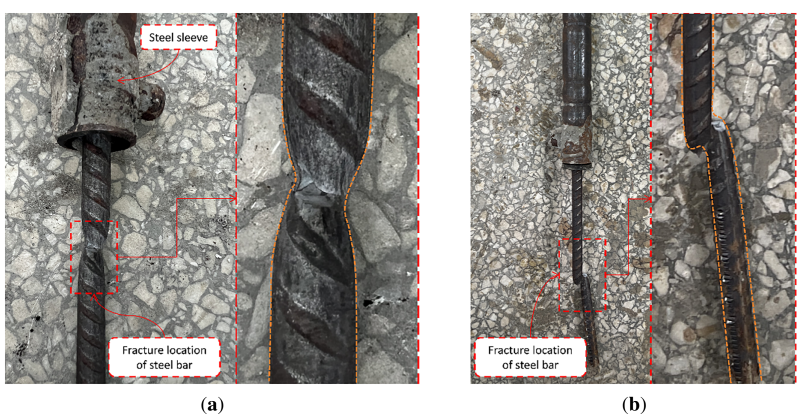

Figure 6: Tensile fracture of rebar. (**a**) Overall view of the fracture location outside the steel sleeve; (**b**) close-up view detailing the necking phenomenon at the fracture point.

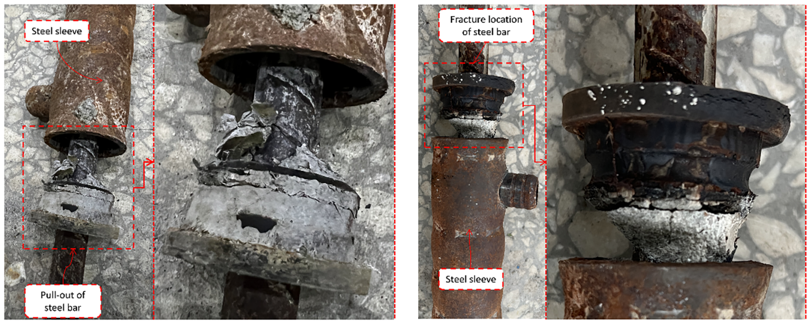

(**a**) (**b**)

Figure 7: Rebar pull-out failure. (**a**) Overall view of the rebar pulled out from the steel sleeve; (**b**) close-up view of the pulled-out rebar and the associated cone-shaped grout failure.

When the test temperature was below 600°C, all specimens experienced rebar tensile fractures. The bond strength between the grout and the rebar was higher than the rebar's ultimate tensile strength, leading to noticeable necking at the fracture point, indicating that the rebar had entered the yielding stage and exhibited typical ductile failure characteristics. This suggests that within this temperature range, the fully grouted sleeve connectors possess good mechanical performance and reliability.

Inside the sleeve, the bonding action between the rebar and the grout is primarily composed of frictional forces and mechanical interlock between their contact surfaces [21]. As the test temperature increased, the bond performance between the rebar and the grout gradually degraded, leading to a reduction in bond strength. Furthermore, the bond stress distribution along the bonded length of the rebar was non-uniform, with higher bond stresses occurring closer to the sleeve ends. When the test temperature reached 600°C, as the tensile force increased to a critical value, the grout at the end of the sleeve experienced cone-shaped failure, followed by the pull-out of the rebar. This type of failure mode is classified as bond failure.

The grout inside the sleeve showed no major damage, indicating that the maximum bond stress was focused at the ends, causing localized grout failure. This also demonstrates the phenomenon of higher bond stress closer to the ends. This type of bond failure only occurred under 600°C conditions. According to the test results, the fracture locations were primarily concentrated outside the sleeve. This is mainly because the cementitious grout inside the sleeve provided a certain protective effect to the rebar, enhancing its residual strength at high temperatures. Consequently, the strength of the rebar segment encased in grout was higher than that of the exposed rebar segment. Therefore, during the loading process, most specimens fractured in the region outside the sleeve.

From a mechanical standpoint, the failure-mode transition observed at 600°C can be interpreted quantitatively as a competition between two capacities: the available bond capacity $F_\gamma = \tau_u \cdot \pi \cdot d \cdot l_a$ and the residual ultimate tensile capacity of the rebar $F_t = f_u \cdot A_s$. When $F_\gamma > F_t$, fracture of the rebar governs and ductile failure is observed; when $F_\gamma < F_t$, pull-out failure governs. Below 400°C, the degradation of $f_0(T)$ is moderate (16% at 200°C and 29% at 400°C) and the bond margin remains positive across all three rebar diameters, in agreement with the observed rebar fractures. At 600°C, however, both $f_0(T)$ (43% reduction) and the bond strength τ_u degrade further, while f_u loses only 10.5%; the resulting collapse of the bond margin manifests as the localised pull-out failures of C80-R12-T600-2, C80-R14-T600-3, and C80-R16-T600-2. This quantitative competition framework, rather than a phenomenological observation alone, provides the rationale for the dimensionless design criterion that is formalised in Section 3.6.

3.4 Load-Displacement Curves

As can be seen from Fig. 8, for specimens that failed by rebar fracture after high-temperature exposure, their load-displacement curves were similar to those of the room temperature specimens. With the exception of the 600°C specimens where the yield stage was not pronounced or had disappeared, they generally experienced an elastic stage, a yield stage, a hardening stage, and a necking-fracture stage. At failure, a clear necking phenomenon was observed at the rebar fracture location, exhibiting typical ductile failure characteristics.

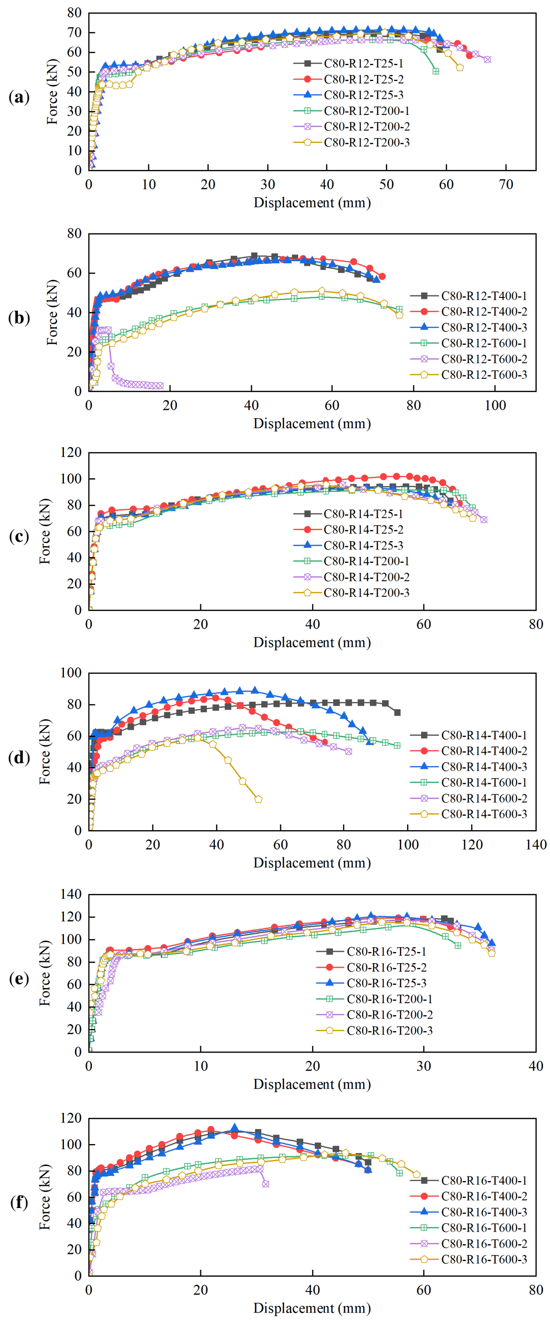

Figure 8: Load displacement curve of sleeve.

For specimens with a pull-out failure mode, the load-displacement curves all showed a distinct elastic stage. After the elastic stage, the three specimens in this study that failed by pull-out exhibited different behaviors, but their tensile deformation upon reaching the ultimate load was significantly smaller than that of the specimens that failed by rebar fracture.

It is evident that the fully grouted sleeve connector specimens tested at 200°C had yield and ultimate displacements that were roughly the same as the room temperature control group. For the specimens tested at 400°C, the yield displacement was slightly greater compared to the control group. As the tensile load increased and the specimens entered the hardening stage, the ultimate displacement increased rapidly. By measuring the specimens after the tensile test and comparing them with the post-test control group specimens, it was found that the increased displacement comprised both displacement from rebar elongation and displacement from slippage between the rebar and the sleeve connector. The displacement from rebar elongation was relatively small, indicating that the elevated temperature adversely affected the bond strength between the grout and the rebar inside the sleeve, leading to slippage between them.

When the temperature reached 600°C, the yield stage essentially disappeared. For specimens that failed by rebar fracture, the displacement increased further. When the failure mode was pull-out, the displacement behavior of the specimens varied. In the case of specimen C80-R14-T600-3*, the hardening stage was not present. After it reached its ultimate strength, the rebar began to pull out, although the bond stress between the sleeve and the rebar had not entirely dissipated, and as the load increased, the rebar was gradually pulled out until failure. Specimen C80-R16-T600-2 showed a long yield plateau after reaching its yield strength. As the load continued to increase, the specimen entered a hardening stage with a gentler slope, and after reaching its ultimate strength, the rebar was gradually pulled out.

3.5 Yield Strength and Ultimate Strength

Table 3 shows that the mechanical properties of fully grouted sleeve connectors at room temperature are similar to those of rebar. At test temperatures of 200°C and 400°C, all specimens experienced failure through rebar fracture. The yield and ultimate loads of each specimen showed a slight decrease compared to those at room temperature (25°C), and all specimens exhibited a distinct yield stage and hardening stage.

As the temperature rose to 600°C, the yield stage of the specimens almost disappeared. Their yield and ultimate strengths decreased more significantly compared to the single rebar specimens, and some specimens exhibited pull-out failure. The failure mode of C80-R12-T600-2 was pull-out failure. After reaching its yield strength, the rebar began to pull out, exhibiting a brittle failure. C80-R14-T600-3 experienced pull-out failure. Once the specimen attained its ultimate strength, the rebar started to be gradually extracted. At this point, some bond strength still existed between the sleeve and the rebar. This bond strength gradually decreased during the pull-out process until the rebar was fully extracted. The failure mode for C80-R16-T600-2 was pull-out failure. After reaching the yield stage and entering hardening, a slip occurred between the rebar and the bonding material. The rebar was then pulled out after reaching ultimate stress.

Directly using the yield load and ultimate load cannot accurately reflect the material strength of the fully grouted sleeve. Therefore, the equivalent stress of the fully grouted sleeve connector is defined using the rebar stress, as shown in Eq. (1).

$$f_y = \frac{4F_y}{\pi d^2}, f_{st} = \frac{4F_u}{\pi d^2} \quad (1)$$

where f_y and f_{st} are the yield strength and ultimate strength, respectively, and, F_y and F_u are the yield load and ultimate load of the specimen. d is the diameter of the rebar within the fully grouted sleeve connector.

When a specimen fails by pull-out, the rebar does not fracture; therefore, the results from specimens that exhibited pull-out failure are not considered. Based on Table 3 and Eq. (1), the equivalent stresses for the sleeve connectors with different rebar diameters at each peak temperature were calculated, as shown in Fig. 9. It can be seen that the corresponding yield and ultimate stresses for the fully grouted sleeve connectors of different specifications are approximately the same under the various temperature conditions. This shows that the specifications of the fully grouted sleeve connector do not impact its mechanical properties. A model for the connector's yield and ultimate stress at various temperatures was created from the experimental results, as reflected in Eq. (2).

$$f_y = \begin{cases} 0.00077t^2 - 0.673t + 471.07, (25°C \le t \le 400°C) \\ -0.30534(t - 400) + 325.07, (400°C < t \le 600°C) \end{cases} \quad (2)$$

$$f_u = \begin{cases} 0.00051t^2 - 0.431t + 624.68, (25°C \le t \le 400°C) \\ -0.38295(t - 400) + 533.88, (400°C < t \le 600°C) \end{cases}$$

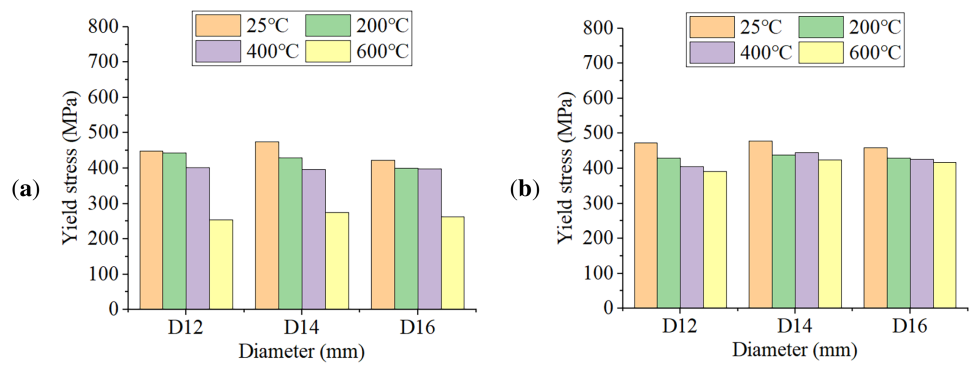

Figure 9: (**a**) Yield stress and (**b**) ultimate stress of the sleeve connectors.

The experimental average values for the yield and ultimate stress of the fully grouted sleeve connectors at each peak temperature, along with the predicted values from Eq. (2), are presented in Table 4. It is evident that there are some discrepancies between the fitted results and the experimental data, but overall, the model provides a good fit. However, it must be acknowledged that the proposed predictive models (Eq. (2)) are primarily empirical and are derived based on the specific specimen configurations and experimental conditions of this study. Due to potential variations in grout properties, sleeve geometries, and thermal protocols in different research contexts, the current model may have certain limitations in terms of broad generalizability. It serves as a preliminary tool for evaluating the high-temperature performance of the specific connectors tested herein.

To assess the predictive accuracy of Eq. (2) more rigorously, the coefficient of determination (R^2) and the maximum relative error were computed against the four experimental temperature levels. The piecewise model achieves R^2 = 0.94 for yield stress and R^2 = 0.91 for ultimate stress, with maximum relative errors of 11.8% (yield) and 6.6% (ultimate). The largest residual occurs at 200°C and is associated with experimental scatter in the yield response of the C80-R12 group. The piecewise structure, anchored at 400°C, is not arbitrary: it coincides with the C–S–H dehydration window identified in Section 3.1, so the transition has both statistical and physical justification. Compared with the single-curve continuous models commonly used in earlier studies of grouted sleeve connections after high temperature, the present formulation captures the regime change at the 400°C threshold without sacrificing simplicity, which is the main novelty of the analytical part of this work.

Table 4: Experimental and predicted values for specimens at different temperatures.

Temperature (°C)	f_y Experimental Average (MPa)	f_y Predicted Value (MPa)	f_u Experimental Average (MPa)	f_u Predicted Value (MPa)
25	449.16	455.63	610.62	614.22
200	424.59	374.47	598.05	558.88
400	398.88	339.47	567.53	533.88
600	264	264.00	457.29	457.29

3.6 Bond Stress

When specimens fail by pull-out after high-temperature exposure, the ultimate load represents the bond force between the sleeve and the rebar. According to research by Zhang et al. [22], the ultimate bond force after high-temperature exposure is as follows:

$$F_u = \tau_u(T)\,\pi d l_a \tag{3}$$

with

$$\tau_u(T) = k\sqrt{f_c(T)} \tag{4}$$

where F_u is the ultimate bond force, l_a is the bond length of the rebar, and d is the rebar diameter. $\tau_u(T)$ is the bond strength between the rebar and the sleeve, where T is the temperature. $f_c(T)$ is the compressive strength of the grout after high-temperature exposure.

Based on the experimental results, the calculation method for the coefficient k is as follows:

$$k = \frac{F_u(t)}{\pi d l_a \sqrt{f_c(t)}} \tag{5}$$

In this study, specimens C80-R12-T600-2, C80-R14-T400-3, and C80-R16-T600-2 failed by pull-out. The corresponding k-values were calculated using Eq. (5) and are shown in Table 5. When the k-value is greater than 1.79, pull-out failure of the sleeve connectors can be prevented. In engineering applications, it is crucial to avoid this failure. Therefore, the bond strength must be high enough to exceed the ultimate tensile strength of the rebar. It should be noted that the coefficient k is derived from only three specimens, which is a relatively small sample size. This value is a preliminary estimate and may involve statistical uncertainty. Further tests with a larger number of samples are necessary to validate and refine this parameter in the future.

Table 5: k-values for sleeve connector specimens at high temperatures.

Specimen ID	F_u (kN)	d (mm)	l_a (mm)	f_c (MPa)	k
C80-R12-T600-2	31.25	12	97	49.27	1.22
C80-R14-T400-3	58.82	14	113	49.27	1.69
C80-R16-T600-2	81.58	16	129	49.27	1.79

To position the proposed criterion within the existing literature, the present k-values are compared with those that can be inferred from related studies. Zhang et al. [22], working on fully grouted sleeves at elevated temperatures, reported bond-stress data that, when normalised by the residual grout strength, yield equivalent k-values broadly clustered around 1.6–1.7 at 600°C. Zhu et al. [18], for semi-grouted sleeves, suggested somewhat lower equivalent values owing to the different load-transfer mechanism. The boundary value k = 1.79 identified in this work therefore lies on the conservative side of the data range reported for fully grouted sleeves and provides a single, dimensionless quantity that is straightforward to embed into design clauses for post-fire safety assessment of precast joints. To the best of our knowledge, this is the first time such a closed-form criterion has been proposed specifically for fully grouted sleeves after fire exposure, which constitutes the principal engineering contribution of this work. The acknowledged limitation regarding the small pull-out sample size remains, and a broader experimental campaign is planned to refine the bound and to extend the criterion to grouts of other strength grades.

4 Conclusions

This study conducted static tensile tests on 36 fully grouted sleeve connectors and 36 single rebar specimens, with test conditions including room temperature and high temperatures of 200°C, 400°C, and 600°C. The main research findings are as follows:

(1) The compressive strength of the grout decreases with higher temperatures, with reductions of 16% at 200°C, 29% at 400°C, and 43% at 600°C. The yield and ultimate strengths of the rebar also decline, with about 17.2% and 10.5% reductions at 600°C.
(2) The failure mode changes with temperature. Below 600°C, all specimens failed due to rebar fracture, showing ductile behavior. At 600°C, some specimens experienced pull-out failure, indicating a loss of bond strength at the rebar-grout interface.
(3) Load-displacement curves show that specimens tested below 400°C pass through complete elastic, yielding, and hardening phases. At 600°C, the yield phase is diminished or absent, leading to significant increases in displacement, showing the negative effects of high temperature on the bond between rebar and grout.
(4) The yield and ultimate stresses of connectors with different rebar diameters (12, 14, and 16 mm) are generally consistent at the same temperature, indicating that sleeve specifications do not greatly affect mechanical performance. A predictive model for yield and ultimate stress was developed, effectively estimating residual capacity for post-fire assessments of precast structures.
(5) A method to calculate the bond strength parameter k was proposed based on pull-out failures. When k is greater than 1.79, pull-out failure after high-temperature exposure can be effectively prevented, providing a useful guideline for avoiding bond failures in engineering design.

In summary, the principal contributions of this work, beyond the headline experimental observations, lie in (a) the synchronised testing of grout cubes, single rebars, and fully grouted sleeve connections on the same thermal histories, which makes the bond-vs.-material decoupling possible; (b) the piecewise predictive model anchored at 400°C, which couples the regression with the C–S–H dehydration window and yields R^2 values of 0.94 and 0.91 for yield and ultimate stresses, respectively; (c) the explicit, dimensionless design criterion $k > 1.79$ for preventing pull-out failure of fully grouted sleeves after high-temperature exposure; and (d) the experimental confirmation that, within the 12–16 mm rebar range, the post-high-temperature mechanical response is statistically diameter-independent, allowing unified treatment in design practice. These contributions are intended to be directly usable in the fire-resistant design and post-fire safety assessment of precast concrete structures.

Acknowledgement: Not applicable.

Funding Statement: The author received no specific funding for this study.

Availability of Data and Materials: Some or all data, models, or code that support the findings of this study are available from the corresponding author upon reasonable request.

Ethics Approval: Not applicable.

Conflicts of Interest: The author declares no conflicts of interest.

References

1. Alias A, Zubir MA, Shahid KA, RAhman ABA. Structural performance of grouted sleeve connectors with and without transverse reinforcement for precast concrete structure. Procedia Eng. 2013;53:116–23. doi:10.1016/j.proeng.2013.02.017.
2. Zhang R, Zhao X, Jin L, Du X. Effect of elevated temperature on the low-velocity impact performances of GFRP reinforced concrete slabs. Constr Build Mater. 2023;395(5):132285. doi:10.1016/j.conbuildmat.2023.132285.
3. Wang Y, Wang G. Numerical simulation method for quantitative assessment of fully-grouted sleeve connection damage state and performance under thermal coupling. Int J Therm Sci. 2024;197:108789. doi:10.1016/j.ijthermalsci.2023.108789.
4. Chen D, Peng S, Hui Y, Tam VW, Wang W, Li L, et al. Post-fire mechanical properties of full-grouted sleeve connection with different grouting defects. Case Stud Constr Mater. 2024;21(11):e03616. doi:10.1016/j.cscm.2024.e03616.
5. Zhang J, Xie X, Wang J, Zhou Y, Wang A, Yi W. Influence of elevated temperature on the performance of pre-damaged grouted sleeve connections under tension and compression. Constr Build Mater. 2025;505(11):144690. doi:10.1016/j.conbuildmat.2025.144690.
6. Wang Y, Wang G, Li Y. Numerical simulation and analysis of fully-grouted sleeve connection and two special points at elevated temperatures. Constr Build Mater. 2022;360(2):129589. doi:10.1016/j.conbuildmat.2022.129589.
7. Liang X, Wang J, Wang Y, Xiang H, Feng Q, Xu R. Analytical model of grouted sleeve connector and its solution based on the state space method. Constr Build Mater. 2022;341(4):127708. doi:10.1016/j.conbuildmat.2022.127708.
8. Li Q, Yi M, Zhang B. Mechanical properties of grouted sleeve splice with horizontal grouting defect after exposure to high temperature. Structures. 2025;79:109443. doi:10.1016/j.istruc.2025.109443.
9. Liu Q, Li J, Li M, Wu X, Li Y, Zhang L. Bond performance prediction model of defective grout in post-fire sleeve connections under cyclic loading. Constr Build Mater. 2023;400(1):132442. doi:10.1016/j.conbuildmat.2023.132442.
10. Wang T, Zhou Z, Yuan K, Jiang R, Ma X, Li L. Evaluation of common defects of grouted sleeve connectors. Case Stud Constr Mater. 2022;17(1):e01605. doi:10.1016/j.cscm.2022.e01605.
11. Wang W, Li JH, Guo F, Chen P. Comparison of tensile mechanical properties of half grouted sleeve connection at elevated and post-elevated temperature: an experimental study. Constr Build Mater. 2024;433(55):136723. doi:10.1016/j.conbuildmat.2024.136723.
12. Lai M. Impact of tunnel fire and high ground temperature on the durability and thermal damage mechanism of structural materials. Appl Comput Eng. 2025;117(1):23–8. doi:10.54254/2755-2721/2025.19955.
13. Ma J, Zhu J, Guo D. Study on pull-out test of steel and semi-grouting sleeve connection after high temperature. Struct Concr. 2025;26(2):1176–89. doi:10.1002/suco.202301095.
14. Liu Y, Peng T, Miao J, Liu C, Ba G, Zhao Y, et al. Uniaxial tensile behavior of half-grouted sleeve connections with concrete cover after exposure to elevated temperatures. J Build Eng. 2024;87(5):109066. doi:10.1016/j.jobe.2024.109066.
15. Li Y, Cheng L, Lei W, Su Y, Huang T, Zhu Y, et al. Microstructures and mechanical property of post-fire grouting sleeve connections considering concrete cover. Constr Build Mater. 2023;403(5):132578. doi:10.1016/j.conbuildmat.2023.132578.

16. Yi M, Li Q, Wu K, Shen Y. Mechanical properties of the grouted sleeve splice with different anchorage lengths after exposed to elevated temperatures. Constr Build Mater. 2025;490:142644. doi:10.1016/j.conbuildmat.2025.142644.
17. JG/T 398-2019. Grout-filled coupling sleeves for rebars splicing. Beijing, China: Ministry of Housing and Urban-Rural Development of the People's Republic of China; 2019. (In Chinese).
18. Zhu J, Ma J, Guo D, Wu Y, Ma J. Study on tensile properties of semi grouted sleeve connectors after high temperature. Constr Build Mater. 2021;302(3):124088. doi:10.1016/j.conbuildmat.2021.124088.
19. Xiong Y, Wu D, Tang Y, Hu M, Shu H. Experimental studies on mechanical properties of corroded steel bars after elevated temperature. Procedia Eng. 2017;210(4):622–9. doi:10.1016/j.proeng.2017.11.122.
20. Qian H, Yan D, Chen S, Chen G, Tian Y, Chen G. Effect of high temperature exposure and strain rate on mechanical properties of high-strength steel rebars. J Mater Civ Eng. 2019;31(11):04019261. doi:10.1061/(asce)mt.1943-5533.0002906.
21. Yu Q, Xu X, You G. Experimental study on bond behavior for ribbed steel bars and grout. J Harbin Instit Technol. 2017;49(5):91–101. (In Chinese). doi:10.1016/j.conbuildmat.2021.124059.
22. Zhang W, Deng J, He C, Zhang J, Yi W. Experiment and analysis on mechanical properties of fully-grouted sleeve connection at elevated temperatures. Constr Build Mater. 2020;244(1):118314. doi:10.1016/j.conbuildmat.2020.118314.